Available online at www.sciencedirect.com
SCIENCE DIRECT®
Journal of volcanology and geothermal research
ELSEVIER
Journal of Volcanology and Geothermal Research 132 (2004) 283–310
www.elsevier.com/locate/jvolgeores

Dyke swarm emplacement in the Ethiopian Large Igneous Province: not only a matter of stress

Daniel Mège [a,*], Tesfaye Korme [b]

[a] *Laboratoire de Tectonique, UMR CNRS 7072, Université Pierre et Marie Curie, Case 129, 4 place Jussieu, 75252 Paris cedex 05, France*

[b] *Geology and Geophysics Department, Addis Ababa University, P.O.Box 81064, Addis Ababa, Ethiopia*

Received 14 August 2003; accepted 16 September 2003

Abstract

In the Tana–Belaya area, western Ethiopia, field data and satellite imagery reveal the existence of two dyke swarms, the NE–SW Serpent-God dyke swarm, and the NW–SE Dinder dyke swarm. Both swarms are thought to have the same age, 30 Ma, and are likely to have contributed to feeding the traps. After a description of the swarms, this paper examines their relationships with the basement structures. The two dyke swarms follow major lithospheric weakness zones. The Serpent-God dyke swarm follows the Pan-African Tulu Dimtu ductile shear zone, and the Dinder dyke swarm follows a large NW–SE-trending Precambrian fracture zone already reactivated during the Mesozoic and Cenozoic as the northern boundary of the Blue Nile Rift. Because the dyke swarms are adjacent but their orientation differs, the stress trajectory patterns during their emplacement were spatially variable at local scale. Therefore, rather than plate-boundary processes, the origin of stress is thought to be primarily related to the Ethiopian plume. Postulating (in the absence of more data relating to the magma chambers that fed the traps) that dyke orientation is the result of an axisymmetric stress field, the location of the stress source can be placed close to Lake Tana, which is the centre of the Ethiopian broad negative regional Bouguer anomaly. The dykes in the Tana–Belaya area provide the first clues to the orientation of the stress field that prevailed in the early history of the Ethiopian mantle plume, and to some of the factors that guided the distribution of the trap feeders.

Keywords: Dyke swarm; Ethiopian Large Igneous Province; stress trajectory; structural inheritance; mantle plume; rifting

1. Introduction

1.1. Dyke swarms

Continental mafic dyke swarms in Large Igneous Provinces (LIP) transmit magma from reservoirs located at the asthenosphere–lithosphere boundary or at shallower depth to the surface where they feed voluminous traps, on the order of 10^5–10^6 km^3 (e.g. Ernst et al., 2001). The composition, age, geometry, palaeomagnetism, flow pattern, and tectonics of dyke swarms in LIPs have been investigated in many other parts of the continental world (review in Ernst et al., 1995). Dyke swarms have been studied not only

* Corresponding author. Tel. +33-1-44272308; fax +33-1-44275085.
E-mail addresses: mege@ccr.jussieu.fr (D. Mège), tkorme@yahoo.co.uk (T. Korme).

0377-0273/03/$ – see front matter © 2003 Elsevier B.V. All rights reserved.
doi:10.1016/S0377-0273(03)00318-4

for locating the eruption sites of flood basalts (e.g. Swanson et al., 1975), but also for the identification of reservoirs, through magma flow direction analysis (e.g. Ernst and Baragar, 1992; Callot et al., 2001) and overgrowth texture patterns (Ohnenstetter and Brown, 1992), as well as for palaeostress trajectory retrieval at various scales on various planets (May, 1971; Féraud et al., 1987; Baer and Reches, 1991; Cadman, 1994; Grosfils and Head, 1994; Mège and Masson, 1996). Dyke swarms are thus key contributors to plume tectonics analysis.

As far as the Ethiopian LIP is concerned, the term flood basalt province should be avoided because it incorrectly reflects the composition and emplacement of the lavas erupted in response to the impingement of the Ethiopian plume on the base of the Ethiopian lithosphere, an event that

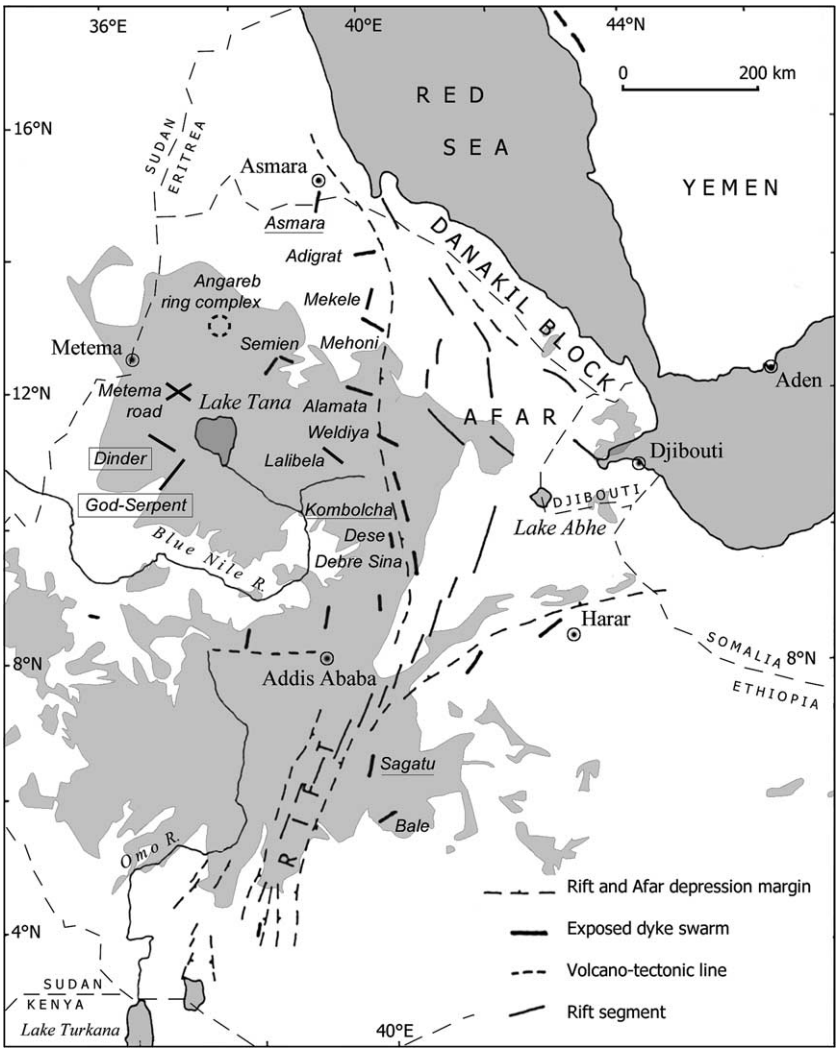

Fig. 1. Location of the main dyke swarms in Ethiopia according to and modified after Mohr and Zanettin (1988). Many dyke swarms reported on this map have not been studied yet, and unreported swarms are likely to exist. Swarm orientations are indicative of the main dyke strikes, although the swarms on the Afar margin display multiple orientations, presumably in response to post-emplacement rotations. Previously studied dyke swarms are underlined (references in the text). The Serpent-God and the Dinder dyke swarms, studied in the present paper, are framed. The Dinder, Metema, Lalibela and Mekele swarms were not included in Mohr and Zanettin's survey. The current exposure of the Trap Series is from various sources.

took place at 30 Ma (Hofmann et al., 1997). The whole lava pile includes basaltic lava flows, basaltic tuffs, as well as a considerable volume of rhyolitic, trachytic, and phonolitic products (e.g. Mohr and Zanettin, 1988). Intermediate volcanic products are scarce but not absent (Mohr, 1963; Mohr and Zanettin, 1988). In this work we use the generic term Trap Series instead of flood basalts for describing the erupted volcanic products at the onset of mantle plume activity.

In the Ethiopian LIP a body of work has been done recently on Trap Series geochemistry and age determination (Hart et al., 1989; Marty et al., 1996; Stewart and Rogers, 1996; Hofmann et al., 1997; Pik et al., 1998, 1999; Ayalew and Yirgu, 2003; Coulié et al., 2003). Several local dyke swarms are exposed (Fig. 1), some of which might belong to the same, thus larger, swarm, but due to the still huge surface area covered by the Trap Series as well as the vegetation cover, exposures are usually not followed over distances exceeding kilometres. East of the East Ethiopian Rift, local swarms are observed on the rift margin and the Bale Mountains. On the rift margin, the Sagatu Ridge dyke swarm has been studied by Mohr and Potter (1976), Mohr (1980), and Kennan et al. (1990). On the northern plateau (Abyssinia), the best known dyke swarm exposures are on the Afar margin and the plain area southwest of Lake Tana, which we call the Tana–Belaya area (Fig. 2). Dykes exposed across the tilted blocks of the Afar margin along the

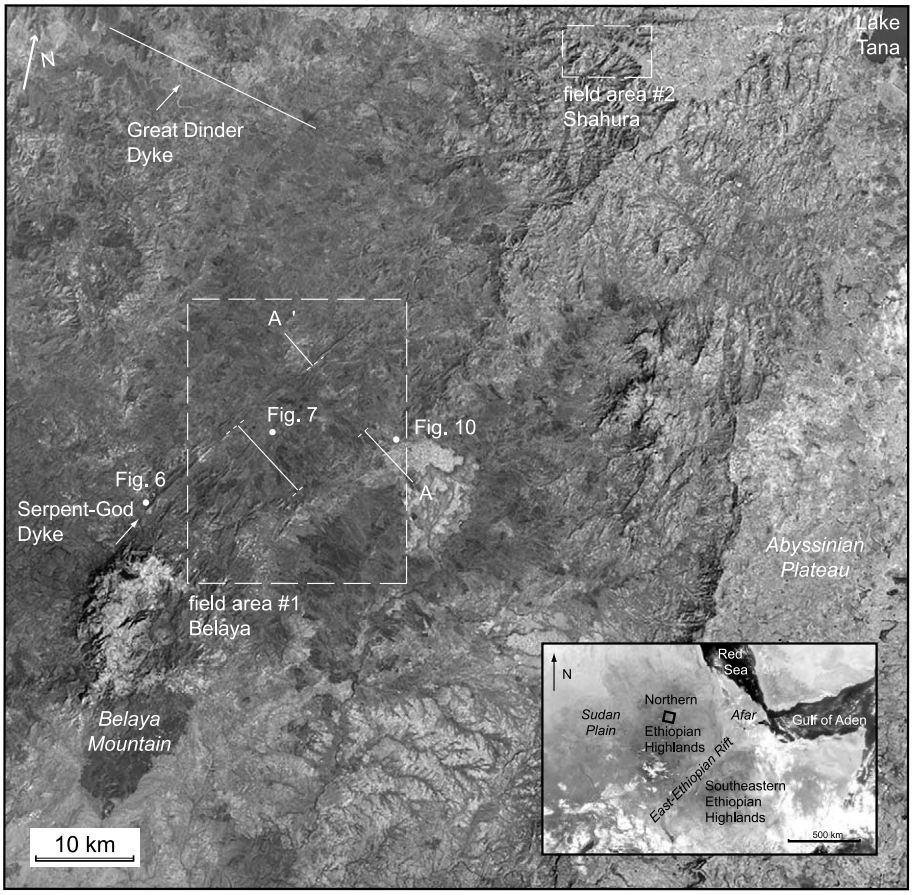

Fig. 2. Part of Landsat ETM+ image KJ170-02 displaying the Tana–Belaya area, the Serpent-God dyke and the Great Dinder dyke, the areas where field work was done, the Serpent-God swarm traverse discussed in the text (AA′), and location of Figs. 6, 7 and 10.

Kombolcha–Bati Road were investigated by Abbate and Sagri (1969), Justin-Visentin and Zanettin (1974), and Mohr (1983). Reconnaissance mapping of dykes in the Tana–Belaya area, western Ethiopia, has been carried out by Jepsen and Athearn (1963a), and satellite imagery interpretation was proposed by Chorowicz et al. (1998).

Other investigated dyke swarms in Ethiopia and Eritrea include the dykes from the Angareb ring complex (Hahn et al., 1977) and the Asmara dyke swarm (Mohr, 1999). Other dyke swarms have been identified (Mohr, 1971; Mohr and Zanettin, 1988, and personal observations), but are still scientifically pristine (Fig. 1).

It is to be expected that most dyke swarms are related to one of the following events: trap eruption, Red Sea opening, or opening of the East African Rift. However, few works have attempted to correlate the dykes with their regional tectonic setting. In this paper, we report on the first field observations of the dykes in the Tana–Belaya area, western Ethiopia, that we complement with satellite imagery. This area was selected due to excellent dyke exposure compared with most other dyke swarms in Ethiopia (Fig. 2). The dyke swarms are identified and described, and their emplacement is investigated, especially in relation to basement fabric. Basement fabric, stress patterns inferred from dyke orientation, and gravity data are combined to put dyke emplacement in the geodynamic context of the Ethiopian plume.

1.2. Known geology of the study area

The Tana–Belaya area is at the convergence of three geologic provinces, the uplifted Trap Series of Abyssinia to the east, the Pan-African orogen, observed to the south, and the Mesozoic–Cenozoic basins in Sudan to the west. The dykes are observed on the Ethio–Sudanese Plain, below the Abyssinian plateau (Plate I). The plain is mainly represented by the Pan-African basement south of Mount Belaya, and the base of the Tertiary Trap Series, made of basaltic flow breccias to the north (e.g. Merla et al., 1979). The plain gradually enters the Sudanese rift domain as one approaches the Ethio–Sudanese border. Alluvial sediments have also been deposited by the Nile and its tributaries.

The Pan-African basement is composed of magmatic rocks (granites, syenites), metamorphosed magmatic rocks (basic metavolcanites) metamorphosed sediments (graphitic schists, phyllites, quartzites, marbles), and also arkoses (Kazmin, 1975; Kazmin et al., 1978; Berhe, 1990; Braathen et al., 2001). It displays a ductile shear zone, the Tulu Dimtu shear zone, of mean orientation NNE (Fig. 3). The shear zone exhibits several ophiolite exposures, usually called the Tulu Dimtu ophiolite belt, one of the several Pan-African ophiolite alignments identified from Tanzania to Egypt and Sudan to Arabia (Shackleton, 1979, 1986; Vail, 1985; Berhe, 1990; Abdelsalam and Stern, 1996), and dated 800 Ma or younger (Berhe, 1990). Elevation maps of the Precambrian basement in Ethiopia were published by Dainelli (reproduced in Baker et al., 1972, p. 11) and, more recently, Beyth (1991). Quaternary lava flows have been observed to lie directly on the Precambrian basement (Jepsen and Athearn, 1962), and on the bottom levels of the Trap Series (field observations by the authors).

The Abyssinian plateau is composed of the Tertiary Trap Series, Miocene shield volcanoes such as the Semien (Mohr, 1967) and Choke Mountains, and Quaternary volcanics. A review of trap stratigraphy throughout Ethiopia can be found in Pik et al. (1998). The total volume of erupted traps in the Ethiopian LIP was estimated to be on the order of 400 000 km^3, with an initial surface area of 750 000 km^2 (Mohr and Zanettin, 1988). Trap thickness reaches up to 2000 m in some areas (Jepsen and Athearn, 1962; Hofmann et al., 1997). Recently determined $^{40}Ar/^{39}Ar$ dating in northern Ethiopia has yielded 30 Ma ± a few ka for most of the Trap Series (Hofmann et al., 1997; Coulié et al., 2003; Touchard et al., 2003). This very short time span is consistent with the eruption time span at most other flood basalt provinces. However, the origin of the Ethiopian LIP is not fully understood yet. The age of volcanism has been shown to be as old as 45 Ma in Kenya, an age that appears to decrease northward, where ages as young as 19–12 Ma have been found on the southern Ethiopian

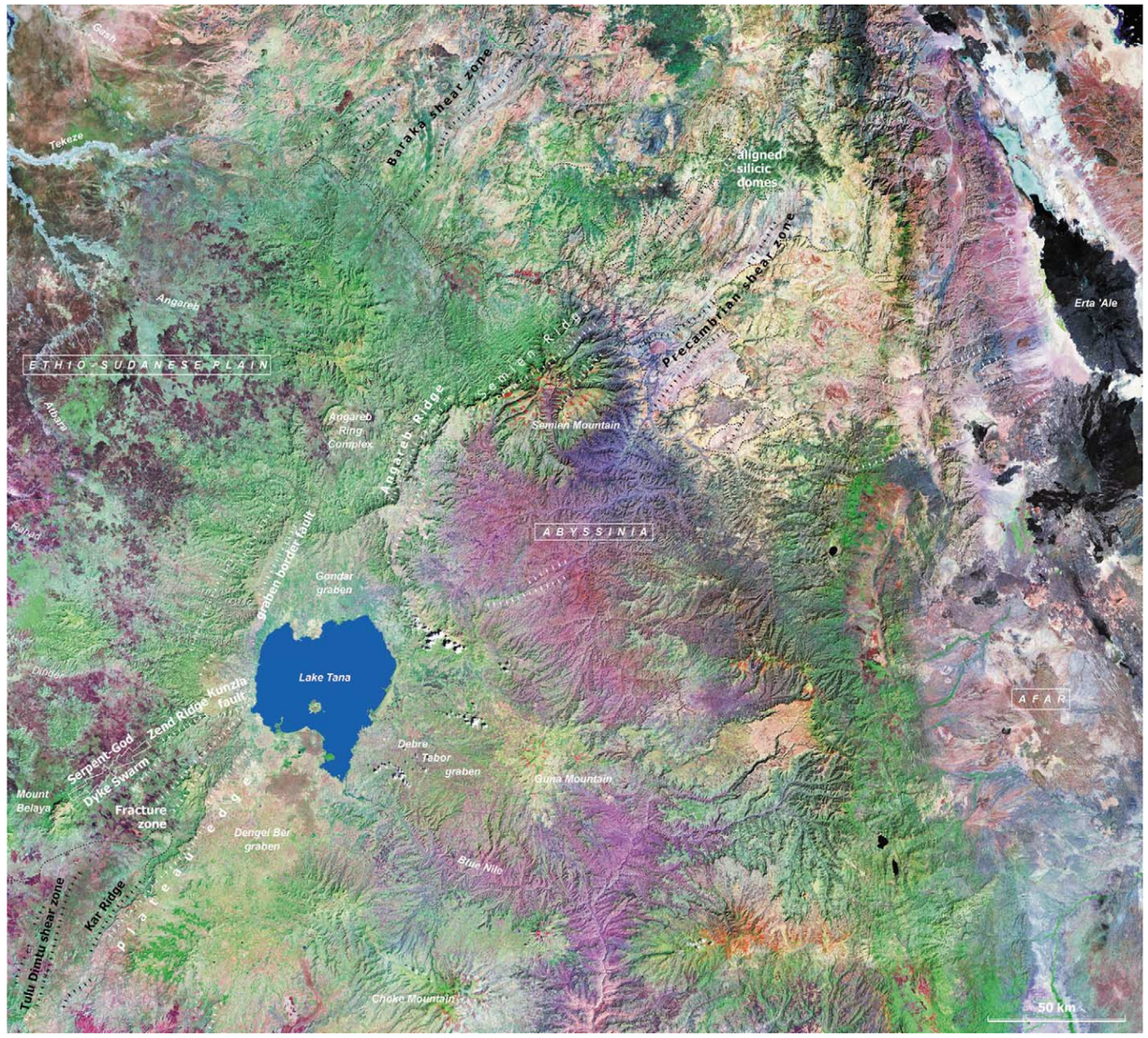

Plate I. Landsat TM mosaic of Abyssinia (bands 741) showing the location of the major NNE to NE–SW structural patterns discussed in the text. Black arrows highlight Precambrian foliation trends; white arrows highlight Cenozoic dykes, fractures, and scarps whose location and orientation are thought to have been controlled by basement structure. Tectonic structures that are not directly related to this study have been omitted for clarity; they can be found on Fig. 3. The black dashed line locally highlights the unconformity between the Precambrian basement and the Trap Series (or Mesozoic sediments conformably underlying the Trap Series). The diagram of dyke trends, which locates the Serpent-God dyke swarm, is from Fig. 5.

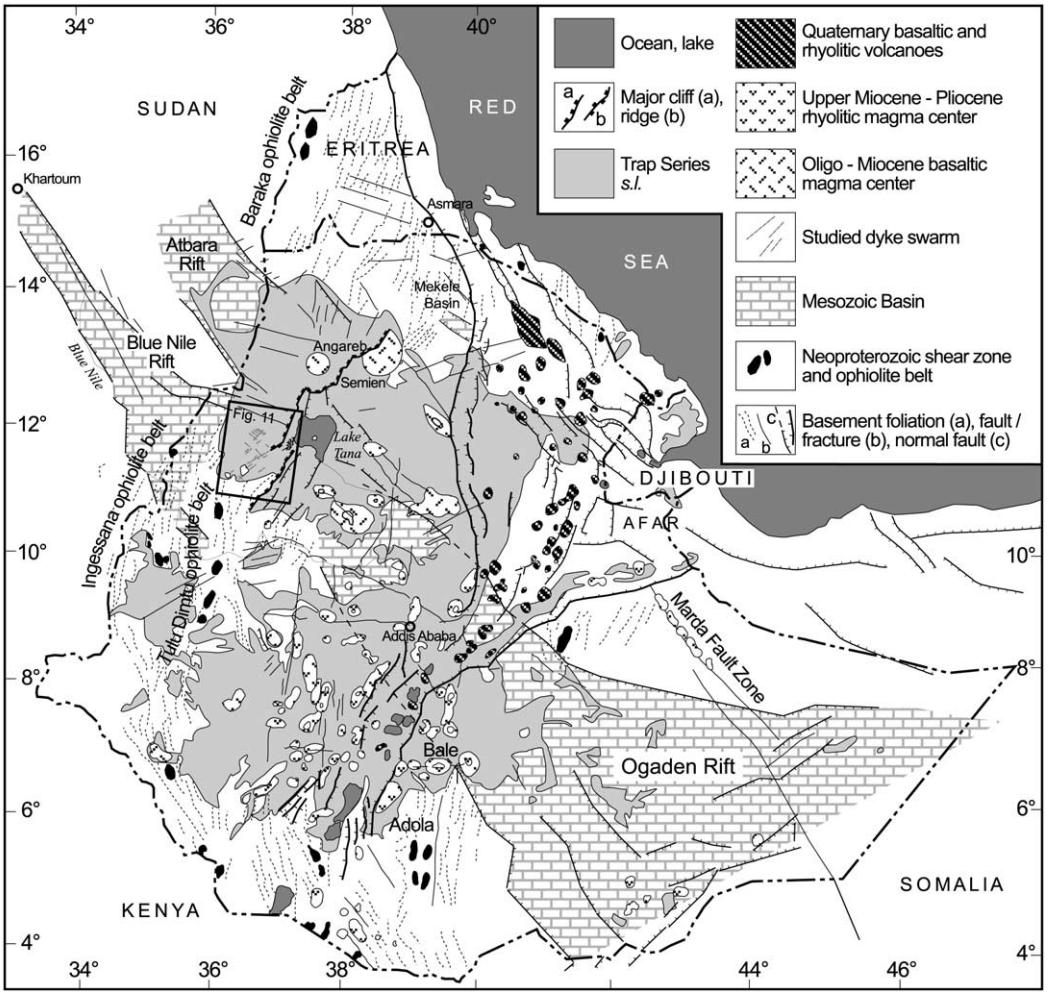

Fig. 3. Structural map of the Ethiopian highlands and peripheral areas, drawn from interpretation of Landsat TM imagery (bands 741) and the published literature.

plateau (George et al., 1998). Late Miocene volcanism has also been documented southeast of the study area, north of Addis Ababa (Zanettin and Justin-Visentin, 1974). Hydrovolcanic craters, Quaternary cinder cones, and related lava flows are also observed (Comucci, 1950; Jepsen and Athearn, 1961). Quaternary cinder cones are observed on the plateau southwest of Lake Tana at a short distance from the Tana–Belaya area.

The plateau has undergone intense fracturing ascribed to uplift associated with trap emplacement, as well as normal faulting. Field evidence shows waning structural deformation after flood basalt emplacement, although some areas underwent Pliocene–Quaternary uplift exceeding 2000 m (Mohr and Zanettin, 1988). A couple of high intensity historical earthquakes have been reported (Jepsen and Athearn, 1963b).

Coblentz and Sandiford (1994) showed that lithospheric density variations are presently the most likely stress sources in the area. They suggested that the present-day state of stress is extensional, and that the magnitude of extensional stress in the Abyssinian plateau is the highest of the whole African plate. Bosworth and Strecker (1997) determined from borehole breakouts that

the minimum stress trajectory in the Sudanese Plain west of the study area is NNE-oriented, perpendicular to the stress field predicted by Coblentz and Sandiford (1994). Inversion of fault slip data sets on faults located around Lake Tana has suggested that the maximum principal stress axis is vertical and the other principal stresses are horizontal and of equal magnitude, which was interpreted as evidence that the region undergoes active subsidence with little contribution of the regional geodynamics (Chorowicz et al., 1998). Tilted blocks observed on the western edge of Lake Tana (Jepsen and Athearn, 1963b, and Figs. 2 and 11) have been interpreted as a consequence of this subsidence (Chorowicz et al., 1998).

2. Dyke swarm identification

2.1. Method used

The dykes are observed to cut the base of the Trap Series. They have been identified using both field work and analysis of satellite imagery (Fig. 4). The swarms were first identified on satellite imagery, which also proved to be the most reliable method for measuring dyke length and strike. Distinction between dykes and other types of fractures was investigated in the field, as well as dyke composition, thickness, emplacement mechanisms, and structural relationships with the host rock. The dyke map on Fig. 4 was obtained from satellite imagery analysis and field data. The field areas include the Jawi area, NE of Mount Belaya, where the dykes have the highest relief, and the area west of a village named Shahura, west of Lake Tana. Apart from the largest dykes, most dykes could not be followed over large distances due to vegetation and the small number of trails.

The imagery used includes a Landsat ETM+ image of the whole area (6 multispectral channels, resolution 28.5 m/pixel; 1 panchromatic channel, 14.25 m/pixel; and 1 thermal infrared channel, 57 m/pixel), orthophoto maps displaying Spot P mosaics (one panchromatic channel, 10 m/pixel) overlain by Spot stereo-derived digital elevation models, and multispectral ASTER imagery (including three channels of resolution 15 m/pixel). Dyke length is best measured on the Landsat panchromatic channel and ASTER imagery, whereas compositional differences are usually easier to identify on Landsat imagery. Details of dyke identification and length measurements using satellite imagery can be found in Mège and Korme (2004).

Distinction between dykes and other fractures is a major issue in the Shahura field area (Fig. 2) owing to the large number of linear valleys observed to cut the plateau edge. These valleys can result from preferential water flow and erosion along dykes or along other types of fractures. Determining whether these valleys highlight dykes or other fracture types is necessary to place constraints on the boundaries of the swarms observed in the Tana–Belaya area. The issue is also critical for dyke identification in other parts of the Ethiopian traps, where dense networks of parallel structurally-controlled valley networks are frequently observed. Our field work in the study area, as well in other parts of the Ethiopian LIP, suggests that distinction between valleys carved above dykes and above other fracture types cannot be made solely using geomorphological analysis of satellite imagery. Most dense networks of parallel valleys observed in the Trap Series appear not to follow dykes. The dykes that can be observed in the field in such areas are usually not parallel to the valleys, and are hardly identified on satellite imagery because both the dykes and the host rock are of basaltic composition. Specifically, in the Shahura area, a small number of valleys were observed to follow dykes, but in most cases dykes could not be observed. In particular, many E–W fractures are identified on imagery but could not be correlated with dykes in the field.

2.2. Identification of swarms

Statistical analysis of dyke orientation (Fig. 5) shows two preferred dyke trends. NE–SW-trending dykes extend from Mount Belaya, a plateau outlier displaying a 1600-m-thick pile of Tertiary basalts (Mohr and Zanettin, 1988) left after deep erosion along the Beles River and its tributaries (Jepsen and Athearn, 1962), to Lake Tana on the

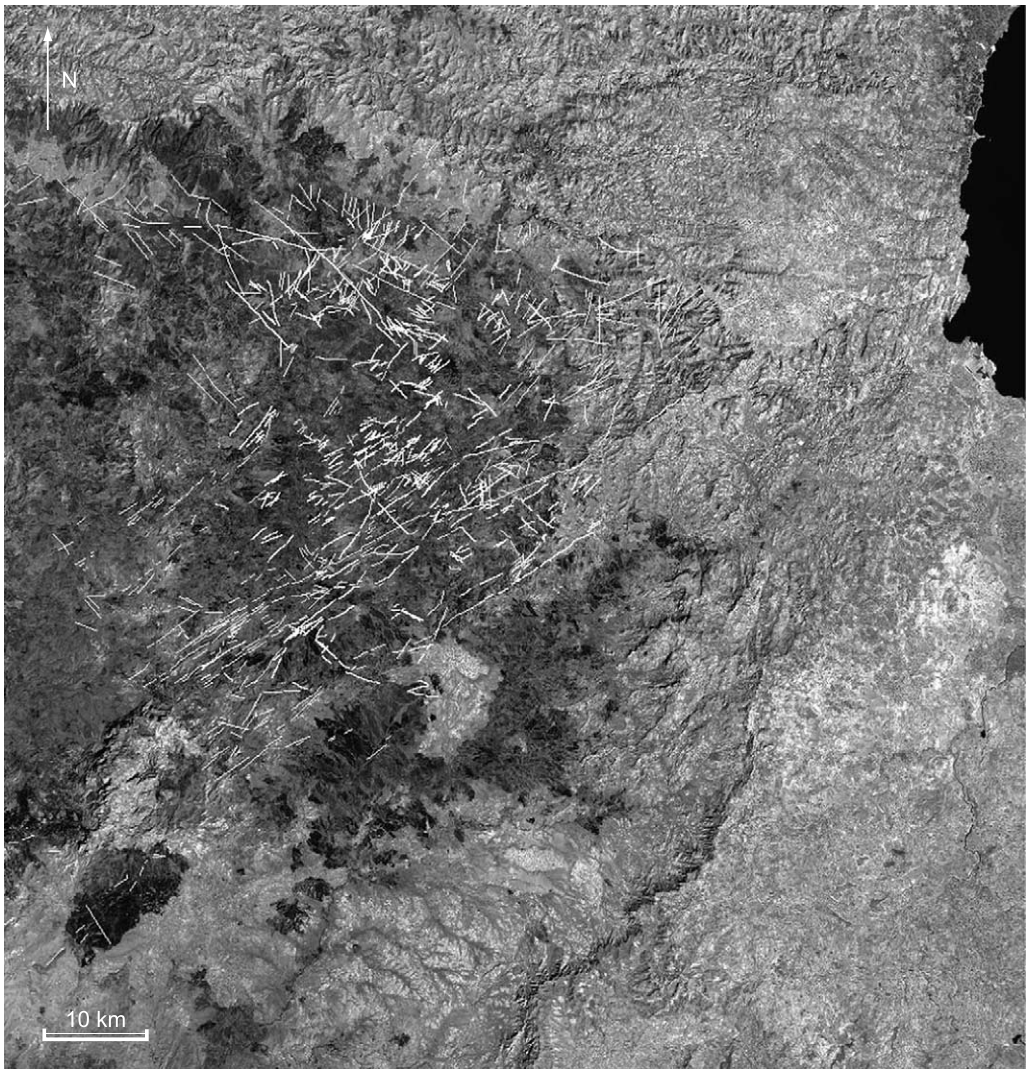

Fig. 4. Dyke location and orientation map in the Tana–Belaya area from satellite imagery and field data. The map is superimposed on the Landsat ETM+ image.

western edge of the Abyssinian plateau. NW–SE-trending dykes are globally observed north of the NE–SW dykes and follow the Dinder River. Therefore, following the usually used geometric criterion, we identify two dyke swarms. The name we ascribe to the NE–SW swarm, the Serpent-God dyke swarm, is from the name local people give to the longest of these dykes (Fig. 2), which also forms the highest topographic relief in the area after Mount Belaya (Fig. 6). The NW–SE-trending dyke swarm has been named the Dinder dyke swarm owing to its alignment with the NW–SE structurally-controlled middle section of the Dinder River, one of the Blue Nile tributaries. Most dykes in the Serpent-God swarm, and all the major silicic dykes, are restricted to a 15–20-km-wide corridor, but the total swarm is more than twice this width. The Dinder dykes appear to be more widely distributed.

In the two field work areas (Fig. 2) most dykes

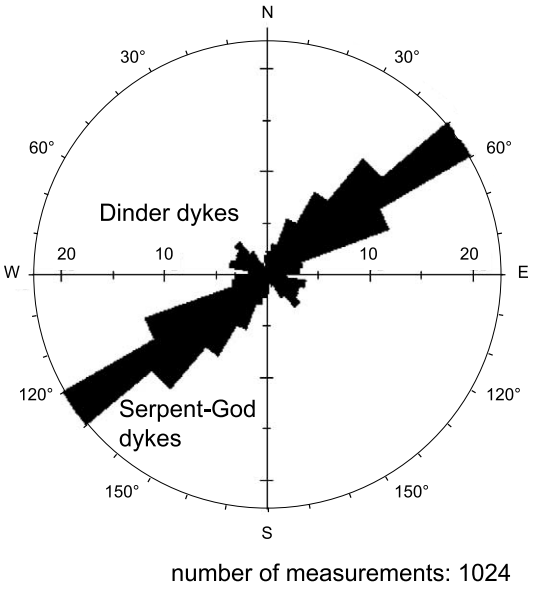

Fig. 5. Dyke orientation in the Tana–Belaya area. The horizontal graduations give the percentage of data within the 10°-wide classes compared to the total number of data. The dykes are plotted on Fig. 4. See Mège and Korme (2004) for a detailed analysis of this diagram.

are parallel, and no cross-cutting relationships could be found that would have allowed a relative emplacement chronology between the swarms to be inferred. Preliminary results of $^{40}Ar/^{39}Ar$ dating (in progress) indicate that the dykes from the Serpent-God swarm are ca. 30.5 Ma old, the same age as the Trap Series in Abyssinia (Hofmann et al., 1997). The Dinder dyke swarm is likely to have the same age as well if it contributed to feed the Trap Series. Quaternary lava flows are not geographically correlated with the location of the Dinder dyke swarm. The shield volcanoes, such as the Semien Mountain, have associated basaltic dyke swarms; however, those swarms are local and observed within the eroded edifices. Such volcanoes have not been identified in the Dinder dyke swarm area, where in addition the dykes rather follow a linear trend and are distributed over a surface area that largely exceeds the size of shield volcanoes. Therefore, it is expected that, similar to the Serpent-God dykes, the Dinder dykes contributed to feed the 30-Ma-old Trap Series.

2.3. Dyke anatomy

Field work has revealed that compositionally the dykes fall into two categories, silicic and basaltic. Composite dykes have never been observed. Of 17 sampled dykes, most have a distinct texture. Frequently, the freshness of the outcrops does not allow inference of their initial composition. The largest of the silicic dykes, the Serpent-God dyke, however, has a microgranitic composition. Silicic dykes form prominent reliefs that are easily identified on satellite imagery. Although dyke thickness is on the order of 10 m and elevation above the surroundings does not usually exceed several metres, they form hills up to 100 m high and hundreds of metres wide owing to the presence of well-developed debris slopes on the dyke sides (Fig. 6). To the contrary, most mafic dykes do not form significant relief. Those of highest relief are observed at the top of bumps that are not more than a few metres high. Mafic dykes crossing river beds form positive relief not more than 1 m high across the river bed (Fig. 7) to linear depressions tens of centimetres deep. Some others form the floor of river beds or, as discussed previously, stream beds. Thus, silicic and basaltic dykes can be easily distinguished on satellite imagery on a geomorphological basis. The reason for this geomorphologic contrast is related to host rock lithology. The host rock includes basaltic breccias, flows, and tuff. The chemical alteration susceptibility of the mafic dykes is therefore in the order of that of the basement. In contrast, the silicic dykes, due to the abundance of resistant minerals such as quartz and feldspar, are globally more resistant to alteration, despite an alteration crust as thick as several tens of cm. The erosional susceptibility contrast between the silicic and mafic dykes and the host rock is also enhanced by the fact that the silicic dykes are systematically thicker than the mafic dykes.

In the field, mean basaltic dyke thickness was found to be 2.7 m, whereas mean silicic dyke thickness was found to be 9.9 m (Fig. 8). Mean basaltic dyke thickness is actually thought to be less because thick basaltic dykes are easier to identify than thin basaltic dykes. The contrast in

Fig. 6. The Serpent-God dyke. Some elder inhabitants in the surrounding villages lay offerings at the bottom of the dyke, which might be a remnant of the pre-Christian Serpent-God worship (e.g. Bader, 2000). According to one of the most widespread versions of the myth, the Serpent-God, 'Arwe, was terrifying the inhabitants in the northern part of Ethiopia and used to be offered maiden ladies as a sacrifice every year. It was killed by 'Angabo, the father of Queen Makeda at ca. 1000 years BC, but the worship is still alive in some remote places in the country. Here the dyke is 20 m thick and is dipping 80°SE. Location on Fig. 2.

thickness between basaltic and silicic dykes is a classical observation that Wada (1994) explains by proportionality between magma viscosity and internal friction. Because high-viscosity magma has high international friction, viscous magma forces the dyke fracture to open wider than mafic, low-viscosity magma can do, resulting in silicic dykes thicker than mafic dykes, all other parameters being equal. A detailed analysis of dyke length can be found in Mège and Korme (in press). The mean length of all the dyke exposures is 1.6 km, and the longest dyke and of globally highest elevation is the silicic Serpent-God dyke (Fig. 2). It displays ~30 major en échelon segments of accumulated length 48 km.

3. Emplacement and post-emplacement history

No feeding reservoir has been identified for the dykes to date. Some of the large shield volcanoes that post-date the Trap Series have a gravity signature (Makris and Ginzburg, 1987); however, the existing gravity data coverage in northern Ethiopia is too sparse to be helpful in the Tana–Belaya area. Field evidence of vertical or lateral dyke propagation, such as phenocryst orientations (e.g. Wada, 1992) was found only exceptionally. Preferential orientation of plagioclases, oriented bubbles, and extrusion striae helped determine magma flow orientation in several instances, but could not be used as a tool to infer regional flow patterns.

Clues to propagation direction may sometimes be inferred from 3-D analysis of dyke segmentation patterns. However, in the field area, due to flatness and the widespread vegetation cover, dyke segmentation could not be interpreted in terms of propagation direction. Small-scale features of dyke segmentation such as epiphyses were usually not observed. In the absence of field evidence, clues to the direction of dyke propagation may be inferred from statistical analysis of dyke length. Mège and Korme (in press) have found suggestions that in the Tana–Belaya area the basaltic dykes longer than ca. 10 km may

have been trap feeders, and therefore should have propagated mainly vertically above the current topography. For the silicic dykes the issue is less problematic because silicic melt density is lower than the density of most plausible host rocks and silicic dykes therefore propagate vertically. The Serpent-God dyke presents evidence of horizontal tip propagation at two adjacent segments (Takada, 1994), but this criterion only gives information on late-stage dyke growth direction at the segment tip.

Several means exist to determine whether the magma was injected into the dykes in one or several pulses. The most favourable case arises when the injection occurs after the previous injection has cooled enough to be chilled by the new magma. Internal chilled margins are a good criterion for determining the number of such injections (e.g. Platten, 2000). Vertical jointing in the dyke parallel to the dyke margins may result from multiple injections (Gudmundsson, 1984). In a case study, Baer (1995) showed on the grounds of magnetic fabric analysis that vertical joints that separate lens-shaped basalt sheets belong to separate injection events. The injection history in that case may be complex and in the absence of magnetic fabric analysis determining the succession of injections is not possible. It can be proposed that cooling joints that are closely parallel to dyke margins are more likely to form within a single magma sheet by gradual magma cooling from the dyke margins inward (Jaeger, 1968) and release of associated tensile stress (Lachenbruch, 1962). To the contrary, a magma injected in a dyke whose

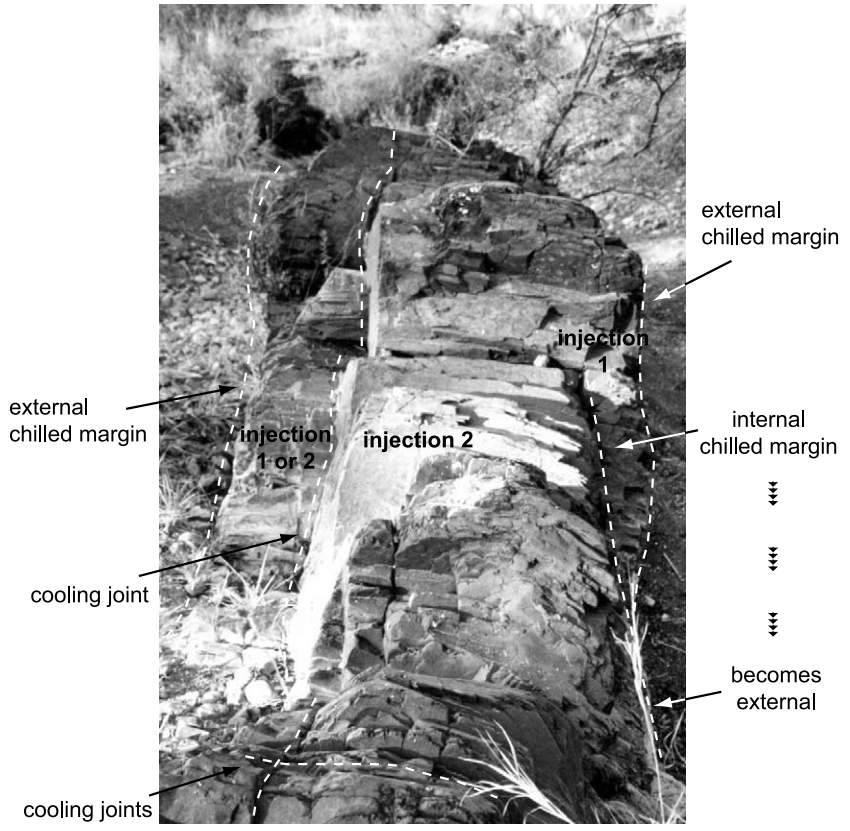

Fig. 7. Basaltic dyke (1.5–2 m thick) in the Ayima River bed. Chilled margins are observed on both dyke sides. Dyke thickness varies at metre-scale in relation with dyke segmentation. The chilled margin on the right side of the dyke in the foreground penetrates within the dyke while a new chilled margin develops outside, suggesting at least two injection stages. On the left side, uncertainty remains as to whether the cooling joint separates or not two injections. Location on Fig. 2.

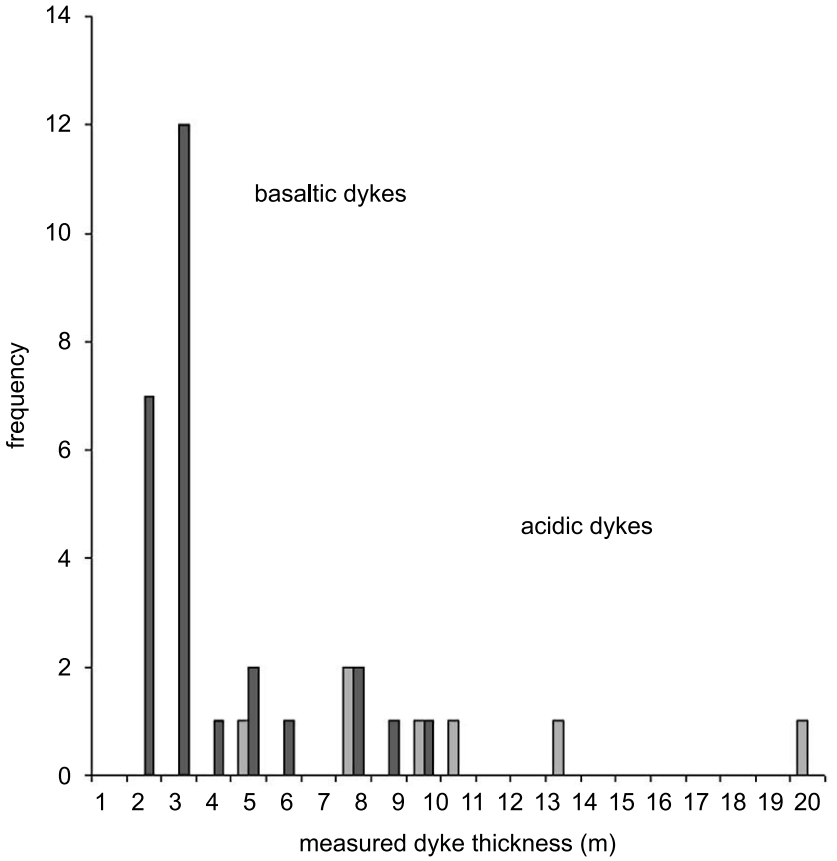

Fig. 8. Histogram of dyke thickness from field observations. Light grey: silicic dykes; dark grey: basaltic dykes.

temperature is still close to the temperature of the arriving magma will probably find its way through the previous magma by deforming it owing to its low elastic modulus. The contact between the successive intrusions will remain a sinuous weakness plane for preferential development of cooling joints, which therefore will be only on a broad-scale parallel to the dyke margins (Fig. 9). In the Tana–Belaya area, external chilled margins are frequently observed, both at silicic and basaltic dykes, but internally chilled margins are observed at a few basaltic dykes only. Detailed examination of those dykes could not reveal more than two injections within the same conduit (e.g. Fig. 7) based on the injection identification criteria in Fig. 9. Internal chilled margins have not been observed in silicic dykes. Thus, the number of magma intruding events within the silicic dykes remains poorly constrained, whereas there is evidence that some mafic dykes as narrow as 1 m thick formed by two injections at least.

How much the dyke injections participated in crustal growth was investigated by measuring dyke dilation along a field traverse across the area of main dyke concentration in the Serpent-God swarm (location on Fig. 2). Table 1 gives the location and thickness of the 28 dykes observed across the traverse. Total measured dilation was found to be 119 m, which equals 0.75% of the 16-km-long traverse. To give an idea, this dilation is two to three times more than the accumulated stretching measured at the Holocene fissure swarms in the eastern Icelandic rift zone (Gudmundsson, 1987). Half the measured dilation is due to the silicic dykes. Given that the silicic dykes form major topographic reliefs and are easily identified in the field, we estimate that total dilation due to the silicic dykes across the whole

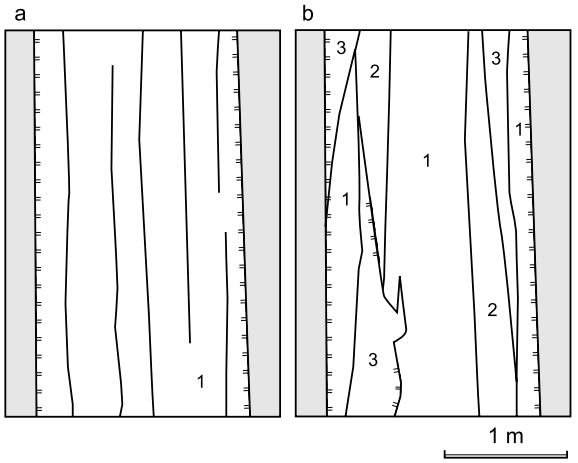

Fig. 9. Suggested difference between vertical joints in dyke induced by (a) gradual cooling inward, and (b) successive flows within the same fissure in horizontal or vertical view. Grey: host rock; plain lines: cooling joints; decorated lines: chilled margins; numbers: injections events. Spacing of cooling joints is more regular if a single injection occurred, and the joints are usually parallel over long distances. Lens-shaped magma sheets suggest more than one injection event even though internally chilled margins are not or seldom observed. Usually there is no field evidence as to the succession of injections within the fissure, but (b) shows a possible example of injection succession. Macroscopic analysis of phenocryst orientations, image processing of thin sections, and analysis of magnetic fabric are tools that may be used to confirm or refute interpretation of such field observations.

swarm is probably close to the actual dilation along the traverse. Dilation due to the basaltic dykes is probably underestimated due to the combined effect of narrowness, weak strength contrast with the host rock, and soil development, which make tenuous the observable difference between lava flows and dykes. A reasonable approximation of true total dilation over the traverse may be 1% or more.

Clues to dyke tilting and brittle shearing along dyke margins or cooling joints after dyke emplacement have been found, but not in an amount that would be sufficient to infer a global tectonic activity framework. Most dykes from the Serpent-God swarm whose dip could be measured are 80–90° dipping, with no preferred dip orientation. At outcrop scale, the dip angle of a given dyke has often been observed to vary between 80°NW and 80°SE. This variation may be ascribed to local along strike variations in elastic modulus in the host rock, and does not imply tectonic tilting. Two prominent segments of the Serpent-God dyke studied in the field showed a consistent 75–80°SE dip (the dip angle of the other segments could not be accurately measured). This feature may result either from local oblique principal stress trajectories, for instance due to body forces associated with uneven palaeotopography, or from post-emplacement tilting.

Several dykes from the Serpent-God swarm, mainly (but not only) the thick silicic dykes, display eroded horizontal slickensides that indicate post-emplacement shearing. For instance, one of the measured basaltic dykes displays clear evidence of dextral shearing parallel to the dyke margin, and later tensile fracturing (Fig. 10). Although a conclusion as to dyke reactivation at regional scale cannot be drawn, field data suggest that limited tectonic activity may have occurred in the study area after dyke emplacement.

4. Basement control on dyke emplacement

4.1. Serpent-God dyke swarm

In order to study the relationships between the dyke swarms and the basement structures, a new structural interpretation of Landsat TM imagery (bands 741) of Ethiopia and eastern Sudan was prepared, on which the Serpent-God and Dinder dyke swarm locations and trends were superimposed (Fig. 3). Mapping reveals that the N055E-trending Serpent-God dyke swarm (Fig. 5) is the northward continuation of the Precambrian Tulu Dimtu shear zone. The orientation of the southern part of the shear zone, which is hundreds of kilometres long, is N–S. Northward, in the southern Tana–Belaya area, its orientation gradually changes to NE–SW, then its continuation is buried by the Trap Series (Figs. 3 and 11).

Continuation of the Tulu Dimtu ophiolite belt on the northern side of the Trap Series is a matter of debate. Shackleton (1979) suggested a possible continuity between the Tulu Dimtu ophiolite and the Baraka ophiolite belt in Eritrea (Fig. 3; Plate I), an interpretation later adopted by Stern et al.

Table 1

Dyke	Thickness (m)	Composition	Latitude	Longitude
D002	20	silicic	N11°39′38.59″	E036°23′28.90″
D006	8.5	silicic	N11°43′06.59″	E036°25′16.30″
D110	13	silicic	N11°36′17.90″	E036°21′55.05″
D113	7	silicic	N11°36′35.95″	E036°21′23.40″
D116	4	silicic	N11°36′06.64″	E036°17′40.36″
D124	6.5	silicic	N11°36′05.69″	E036°19′57.73″
D001	2	basaltic	N11°35′03.99″	E036°28′38.70″
D003	7	basaltic	N11°40′43.49″	E036°24′01.60″
D004	1.3	basaltic	N11°41′10.89″	E036°23′54.20″
D005	7.5	basaltic	N11°41′51.99″	E036°24′42.00″
D102	9	basaltic	N11°28′13.78″	E036°25′56.45″
D103	4	basaltic	N11°34′15.05″	E036°28′28.01″
D104	5	basaltic	N11°34′19.14″	E036°28′14.57″
D105	1	basaltic	N11°34′20.19″	E036°28′12.96″
D106	3.2	basaltic	N11°34′23.55″	E036°28′08.50″
D107	2	basaltic	N11°35′29.46″	E036°24′29.73″
D108	2.5	basaltic	N11°35′30.20″	E036°24′26.67″
D109	2	basaltic	N11°36′11.77″	E036°22′39.30″
D111	1	basaltic	N11°36′24.09″	E036°21′27.77″
D112	0.6	basaltic	N11°36′28.09″	E036°21′25.66″
D114	1	basaltic	N11°36′25.98″	E036°21′20.53″
D115	2	basaltic	N11°36′28.97″	E036°21′17.58″
D117	1.5	basaltic	N11°36′23.64″	E036°17′49.79″
D118	1	basaltic	N11°36′33.49″	E036°17′53.59″
D119	2	basaltic	N11°36′58.06″	E036°17′54.54″
D120	1.2	basaltic	N11°37′12.33″	E036°18′11.85″
D122	1	basaltic	N11°37′11.91″	E036°18′04.27″
D123	2	basaltic	N11°35′58.28″	E036°17′52.32″

(1990). In this hypothesis, the ophiolite belt below the traps must be N–S trending. The map of Vail, 1985 shows the northwestern part of the Tulu Dimtu ophiolite belt to be N–S oriented, which is consistent with its continuation as the Baraka ophiolites, whereas its northeastern part is given a NNE to NE–SW orientation (see also Vail, 1976). Kazmin et al. (1978) suggested that the Tulu Dimtu ophiolite belt broadens or divides into two branches south of Mount Belaya, one going to the north and the other one to the NNE. Shackleton (1988), however, questioned the interpretation of continuous ophiolite belts in the African Horn. Nevertheless, despite the apparent absence of a detailed comparison between the two ophiolite belts, continuation of the Tulu Dimtu ophiolite belt toward the Baraka ophiolite has not been further discussed (Stern, 1994; Tadesse, 1996; Abdelsalam and Stern, 1996; Braathen et al., 2001).

Our own mapping suggests that the Tulu Dimtu shear zone broadens northward with its western border trending N and its eastern border trending NE. The western part of the shear zone appears first to join the Ingessana shear zone, then the Baraka ophiolite near the border with Eritrea (Berhe, 1990). The eastern, NE–SW-oriented border of the Tulu Dimtu shear zone is buried in the Tana–Belaya area, and mapping (Fig. 3) suggests that it joins the shear zone observed north of Semien Mountain.

Figs. 3 and 11 next to Plate I show that not only has the Serpent-God dyke swarm the same orientation as the northern Tulu Dimtu ophiolite belt, but also both are aligned with a series of structural and geomorphological structures that

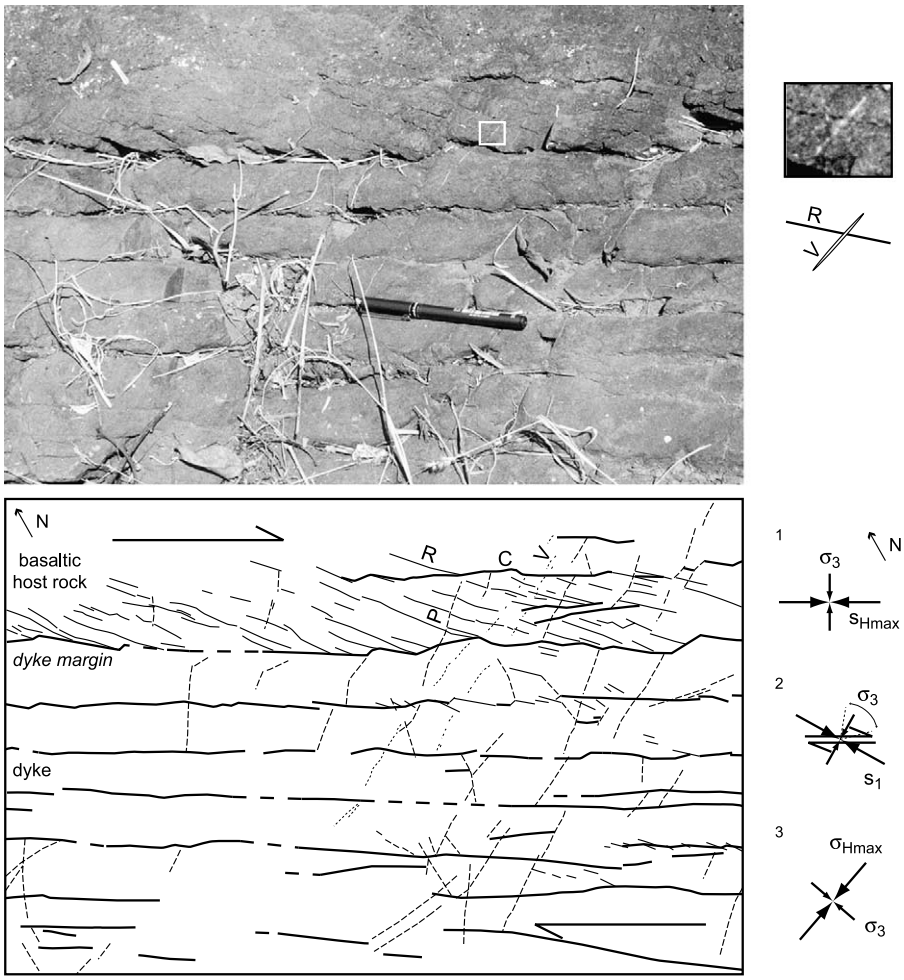

Fig. 10. Close-up view of a 2–3-m-thick basaltic dyke (Mège and Korme, 2004, fig. 6) displaying dextral shearing parallel to the dyke margins and subsequently tension fracturing. Shearing occurred through C/S planes in which C are some of the cooling joints that are parallel to the dyke margin, and S shears are Riedel (R) shear joints. P joints may have reactivated cooling joints oblique to the dyke strike. The enlarged area shows the cross-cutting relationships between a Riedel shear (R) plane and a calcite vein segment (V). The stress trajectories succession cartoon sketches the evolution the local stress field (minimum principal stress σ3) during: (1) dyke emplacement; (2) post-emplacement shearing (approximate orientation, the double arrows illustrates the uncertainty in the σ3 trajectory); and (3) calcite vein opening and filling (calcite fibres assumed to be perpendicular to the vein boundaries). Location on Fig. 2.

can be followed northward until the Precambrian basement is again exposed. East of the dyke swarm, the edge of the Abyssinian plateau forms a steep slope several hundreds of metres high approximately parallel (N030E) to the dyke swarm (N055E). Although it usually does not display field evidence of faulting, satellite and aerial imagery show many fractures parallel to the plateau edge on the plateau and in the plain (Plate I, Fig. 12), suggesting that it is also controlled by the basement. Thus, although the dyke swarm and the plateau edge are not strictly parallel, both appear to be controlled by the same weakness zone. North of Lake Tana, the edge of the plateau follows the same N030E orientation. Although the edge does not display evidence of faulting either, it is parallel to the western border fault zone of the Gonder graben, one of the three main gra-

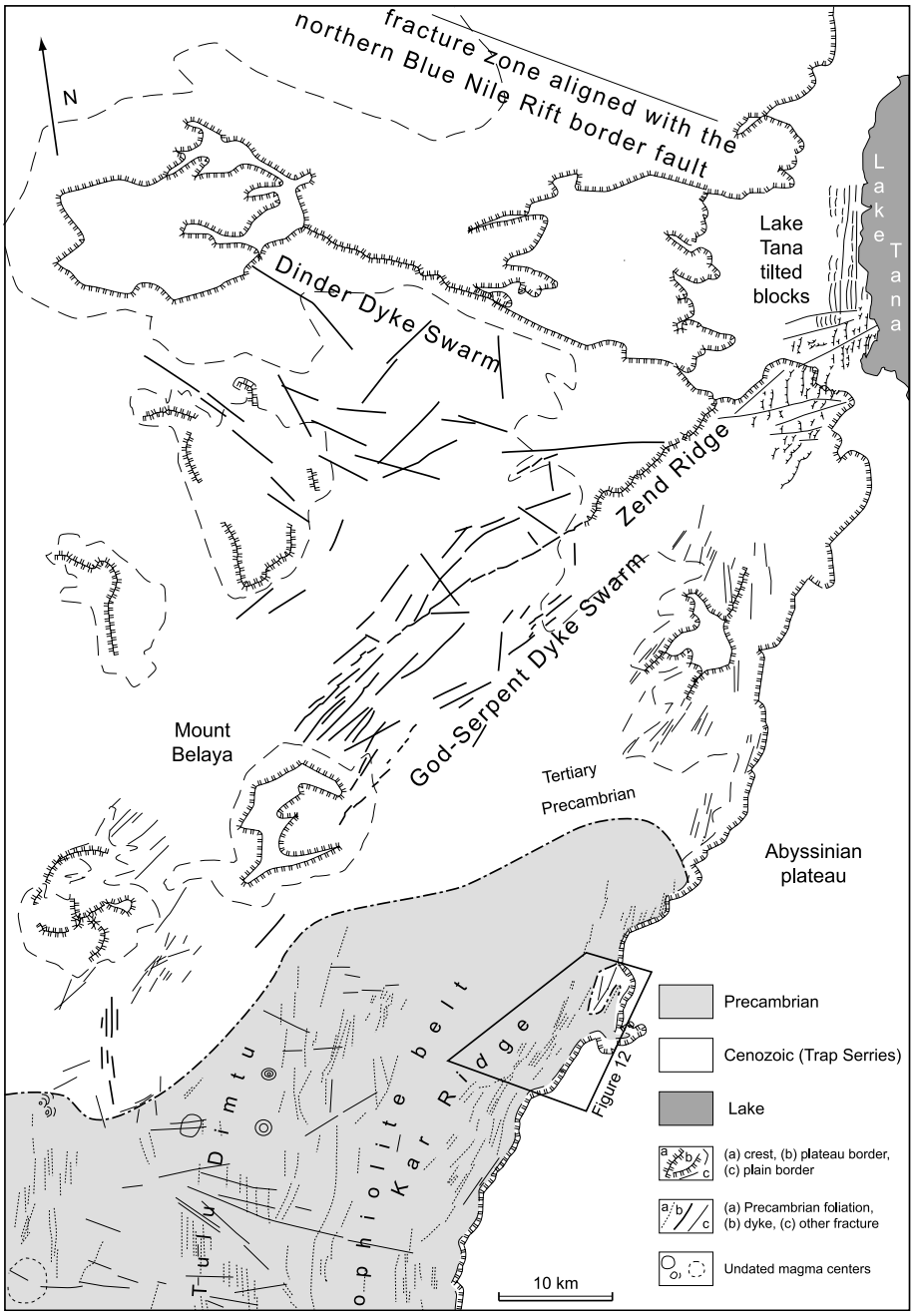

Fig. 11. Structure map of the Tana–Belaya area (location on Fig. 3), showing alignment between the Dinder dyke swarm and the Mesozoic–Cenozoic Blue Nile Rift northern border fault and between the Serpent-God dyke swarm, the Tulu Dimtu Pan-African shear zone and the Cenozoic structures and Quaternary reliefs observed on and in the vicinity of the plateau border. Only the major dykes are located on this map.

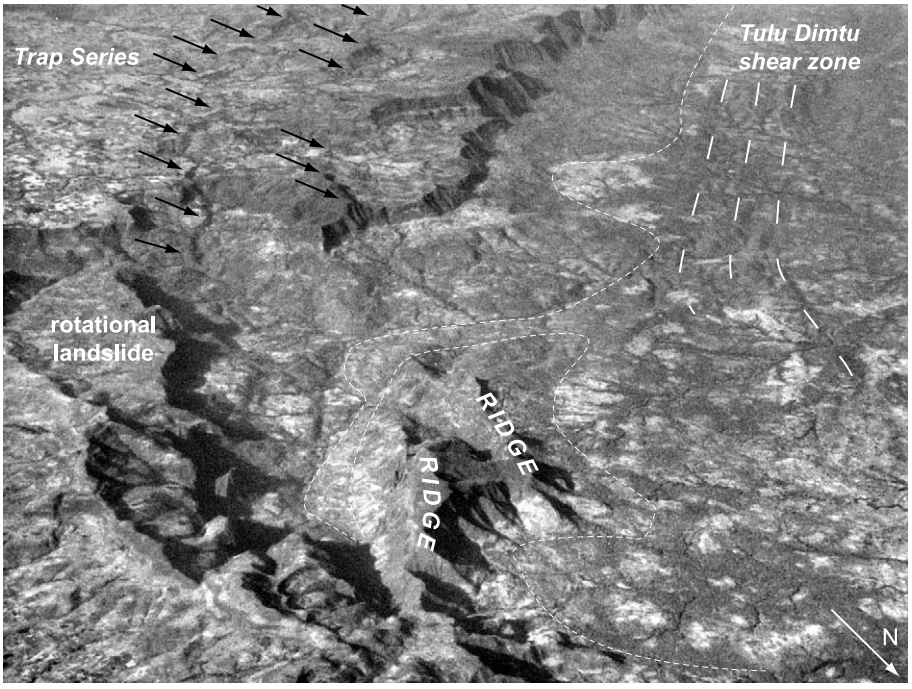

Fig. 12. Aerial view of the plateau edge north of the Kar Ridge. Normal faults are indicated by black arrows. The unconformity between the Tertiary volcanic rocks and the Precambrian basement is outlined by the thin dashed line. The widely spaced dashes follow the Tulu Dimtu shear zone. The plateau edge is parallel to the Tulu Dimtu shear zone. Satellite imagery shows that the westernmost ridge and faults are probably the same structure. Location on Fig. 11.

bens around Lake Tana (Fig. 3), and is parallel to a fault zone observed on the plateau slope. East of the Angareb ring complex, the edge of the plateau, unofficially called the Angareb Ridge, clearly follows a series of N030E fractures, some of which are observed to continue southward and cut the edge of the eastern Gonder graben fault scarp. The Angareb Ridge continues as a long narrower linear cliff, the unofficial Semien Ridge, that cuts the northern flank of the Semien shield volcano. The cliff is locally as high as 1 km, and follows a trend that is sensibly parallel to the dyke swarm (N060E). Several other cliffs of lower relief are parallel to the Semien Ridge. Although any of them display field evidence of faulting (Mohr, 1967), the cliffs are parallel to many fractures observed on the northern side of the Semien Ridge (Plate I). Basaltic dykes have been reported in the Semien Mountain (Mohr, 1967; Lebas and Mohr, 1970). Systematic measurements of dyke attitude along the road of the Semien National Park (unpublished work by the authors) has revealed two types of dykes. The first series is composed of N030–N045E oblique dykes, not more than 1 m thick and frequently associated with sills. The second series is composed of N060–N070E vertical and subvertical, 1–3-m-thick basaltic dykes. It is possible that the first dykes are local, whereas the second, which are parallel to the regional trend of the Semien Ridge, are of regional extent and make some of the fractures observed north of the Semien Ridge on satellite imagery (Plate I). The Precambrian shear zone is exposed NE of the Semien Ridge. Foliation trends are oriented N050E on average, a declination that gradually decreases to N–S toward the North in Eritrea (Fig. 3, Plate I). The general fracture pattern at regional scale between the southern and northern shear zones is thus a series of dominantly N030E segments.

Satellite imagery analysis reveals a second regional structural trend, which we call a tectonic

line below, that is slightly oblique (N060–70E) to the Precambrian foliations. At the northeastern end of the Serpent-God dyke swarm, the dykes are aligned with the Zend Ridge, a major linear crest (Fig. 11, Plate I). The crest is connected with the Lake Tana shoreline by a probably transcurrent fault that transversely cuts across tilted blocks (Chorowicz et al., 1998). Several N060–070E-oriented structural features aligned with the dyke swarm are also discontinuously observed between Lake Tana and the Erta 'Ale in Afar (Plate I). South of Semien Mountain, the tectonic like is marked out by a ridge similar to the Zend Ridge, but on the Afar margin and in Afar it is mainly observed as parallel linear valleys. On Plate I, one of the tectonic line fractures is marked out by a river bed that obliquely cuts across the Precambrian shear zone east of the Semien Mountain. The N060–070E tectonic line is therefore not associated with the events that formed the Tulu Dimtu shear zone.

We deduce that the location of the Serpent-God dyke swarm may have been controlled by the superimposition of two basement patterns oriented ca. 30° apart. One is the Tulu Dimtu ductile shear zone, which is in average N045E-oriented below the Trap Series, the other appear is a N060–70 tectonic line, which probably formed as a brittle deformation zone because of its straightness. Its age is not known. Hypotheses for its formation include: (1) post-orogenic shearing of the Pan-African belt; (2) Mesozoic and Cenozoic rifting (the rift would then be oblique to the NE–SW rifts that opened during this period in the African Horn, including the nearby Mekele graben; Fig. 3); (3) late Cenozoic rifting at the East Ethiopian Rift, which is parallel to the trend of the tectonic line. In that case, the tectonic line would be more recent than the 30-Ma-old Serpent-God dyke swarm and could not have influenced its location.

4.2. Dinder dyke swarm

The Dinder River, in the Tana–Belaya area and north of it, is controlled by Precambrian NW–SE strike-slip faults. The whole Arabian–Nubian shield is affected by large fractures having this orientation (e.g. Kazmin et al., 1978; Adamson and Williams, 1980; Berhe, 1990).

The dyke swarm is aligned with structurally controlled sections of the Blue Nile River and with some of its tributaries, the major ones being the Dinder and Rahad rivers (Fig. 3). The Precambrian fracture zone that controls the course of these rivers was reactivated during the Mesozoic and Cenozoic as the northern border fault of the Blue Nile Rift (e.g. Salama, 1997). At the proximity of Khartoum, this fault is occupied by the Blue Nile River bed. Southeastward, it controls the trend of the Rahad River as far as the Sudan border. At this location, the fault is correlated with a NW–SE-trending negative gravity anomaly (Ibrahim et al., 1996) which is clearly distinct from the Blue Nile Rift gravity signature. At the Ethio–Sudanese border, the rift rests against an E–W trending gravity anomaly (Bosworth, 1992).

From this place southeastward, there is no evidence of the fracture zone on satellite imagery over 120 km. In the Tana–Belaya area, however, its existence is revealed by its controls on the Dinder River course. There is structural evidence of continuation of the Blue Nile Rift trend in Ethiopia east of the Dinder River. The Mesozoic and Cenozoic Blue Nile Rift and the late Palaeozoic–Mesozoic Ogaden Rift, which is observed from Somalia to the Blue Nile gorges south of Lake Tana (e.g. Jordan, 1972), are aligned, so that even though all the grabens in these two rifts were not active at the same time, they are geometrically connected. The Blue Nile–Ogaden trend can be followed until the Red Sea and the Gulf of Aden. Several portions of the Red Sea rift, as well as the orientation of the Afar margin in northern Ethiopia and Eritrea (Fig. 3) and the elongation axis of the volcanoes located at the spreading axis of the Red Sea, such as the Erta Ale (Plate I), have the same orientation. The Marda fault Zone in SE Ethiopia and Somalia (Fig. 3) is the southward continuation of this Red Sea axis, and is another major Precambrian boundary that was reactivated in the Mesozoic and Cenozoic (Purcell, 1976) that is aligned with the Blue Nile–Ogaden trend. Furthermore, Tertiary volcanic centres and lava flows aligned along the

Marda Fault show that this Precambrian weakness zone was utilised during the Tertiary as a long, NW-oriented volcanic fissure parallel to the Dinder dyke swarm. There is thus good evidence that the Dinder dyke swarm follows one of the major structural trends of East Africa.

4.3. Lithosphere structure and dyke emplacement

The lithosphere weakening mechanisms are thus of two kinds. In the case of the Blue Nile and Ogaden rifts, the lithosphere was thinned by tectonic stretching. The rifts should have been areas of preferential magma melting by mantle decompression when the Ethiopian plume impinged at the bottom of the lithosphere, as well as deep channels for evacuating the magmatic heat to regions outside the plume centre (Ebinger and Sleep, 1998).

Emplacement of the Serpent-God dyke swarm above a ductile shear zone is unlikely to have been influenced by individual foliation planes. The shear zones can be followed on satellite imagery as periodically spaced ridges oriented parallel to the foliation planes (Figs. 11 and 12, Plate I). The ridges are probably located between zones of maximum strain determined by lithologic successions. These highly strained zones are preferential zones of potential reactivation. Similar to lithosphere thinning, such weakness zones decrease the elastic lithosphere thickness. Using gravity data, Tessema and Antoine (2003) have recently emphasised that the Proterozoic shear zones in East Africa are sufficiently mechanically weaker than the surrounding resistant cratonic areas that they may have influenced the direction of Phanerozoic rift propagation. Given that dyke dilation at depth replaces tectonic stretching at the surface in volcanic rifts, we suggest that the location of the Serpent-God dyke swarm can be similarly explained.

The Tertiary basaltic magmas may have been generated in situ, or have migrated from other sublithospheric areas (Thompson and Gibson, 1991; Ebinger and Sleep, 1998) in response to the arrival of the Ethiopian plume. A fraction of the magmas would have been trapped at the Tulu Dimtu shear zone and along the southeastern portion of the Blue Nile fracture system owing to their weak mechanical properties. A fraction of the magma would have been injected upwards and formed the basaltic dykes. Two mechanisms for generating the silicic magmas can be envisaged. They may have formed by differentiation of the basaltic reservoirs. However, the age of the basaltic and silicic dykes cannot be separated on the basis of $^{40}Ar/^{39}Ar$ dating (in progress), which suggests that a more likely mechanism for silicic magma generation may be crustal melting in shallower reservoirs at the same time the basaltic reservoirs were active. In northern Ethiopia, rhyolite domes that are aligned with the Serpent-God dyke swarm have been given the same age (30 Ma) and show evidence of crustal melting (Ayalew and Yirgu, 2003).

It may be interesting to note that the tectonic boundary highlighted by the Tulu Dimtu shear zone and the N050–070E tectonic line geographically is concordant with a NE–SW-oriented line going through Lake Tana, to the NW of which the magmas of the Trap Series were significantly contaminated by the crust (Pik et al., 1998, 1999).

5. Summary and discussion

This paper reports on the first field and satellite imagery analysis of dykes in the Tana–Belaya

Fig. 13. (a) Outline of the Precambrian weakness zones that controlled dyke emplacement, and location and orientation of the studied dyke swarms. (b) Stress patterns inferred from geometric analysis of dyke orientation, and example of an axisymmetric stress field that would be consistent with the observed dyke distribution and geometry. Such a stress field could result from a pressurised magma body, or body forces associated with topographic uplift and magmatic loading (isostatic or flexural) of the lithosphere. The diameter of the circle with the arrows is arbitrary. The regional Bouguer anomaly is from Makris and Ginzburg (1987). On the lower right is a proposition of anomaly spreading from an initial axisymmetric geometry. The location of Lake Tana and the Red Sea shoreline is drawn for easy location only; none of them existed when the dykes were intruded.

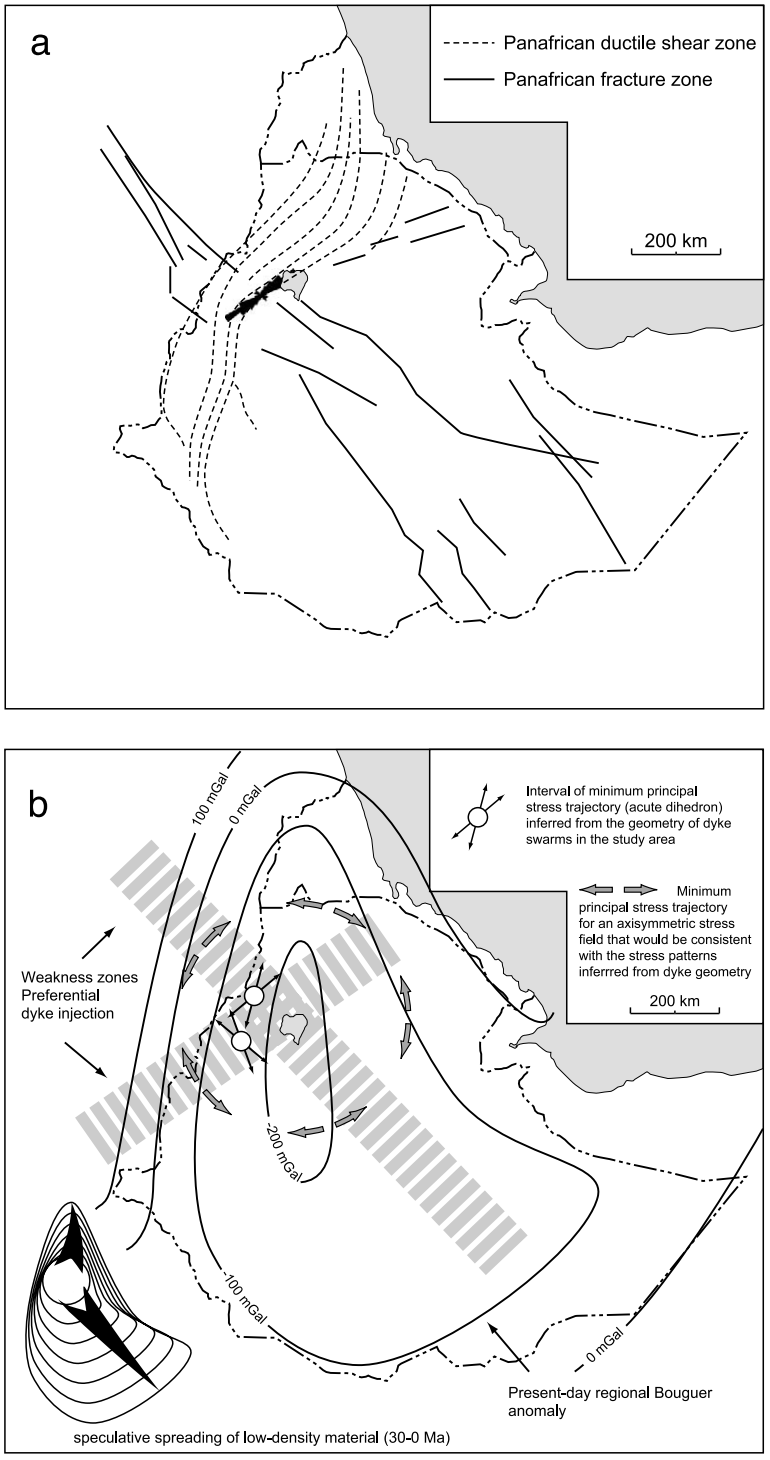
a
Panafrican ductile shear zone
Panafrican fracture zone
200 km
b
100 mGal
0 mGal
-200 mGal
-100 mGal
0 mGal
Interval of minimum principal stress trajectory (acute dihedron) inferred from the geometry of dyke swarms in the study area
Minimum principal stress trajectory for an axisymmetric stress field that would be consistent with the stress patterns inferrred from dyke geometry
200 km
Weakness zones
Preferential dyke injection
Present-day regional Bouguer anomaly
speculative spreading of low-density material (30-0 Ma)

area in western Ethiopia. Earlier works reported either a single, NE–SW-oriented dyke swarm (e.g. Mohr and Zanettin, 1988), or a dyke swarm that would be part of a radial network about Lake Tana (Chorowicz et al., 1998). Statistical analysis carried out in this paper appears to favour the hypothesis that two distinct swarms exist, one N040–070E and the other N105–140E. Most dykes are mafic, but the longest and thickest are silicic. Total dilation across the N040–070E-trending Serpent-God swarm is found not to exceed 200 m at the exposed structural level.

5.1. The studied dyke swarms as compared to other dyke swarms associated with mantle plumes

Clearly, the dyke swarms identified here present several differences with the dyke swarms usually observed in other LIPs. The basaltic dykes in the Tana Belaya are much shorter and thinner than most basaltic dyke swarms associated with mantle plumes, which typically have lengths of hundreds of kilometres and thicknesses of tens of metres. The crustal level exposed may in part explain this difference. In contrast with most dyke swarms associated with mantle plumes, erosion in the Ethiopian LIP has not removed more than 1 km from the initial topographic surface. This is much less than the amount of erosion in regions displaying older dyke swarms (e.g. Baragar et al., 1996), even for Mesozoic dykes (Callot et al., 2001). Basaltic dyke thickness gradually decreases to 0 between the level of neutral buoyancy and the surface. The studied dyke swarms are likely to be observed above the level of neutral buoyancy (e.g. Wilson and Head, 1994), in contrast to most currently exposed dyke swarms associated to mantle plumes. If portions of the studied dyke swarms are still buried by the Trap Series, or are exposed but not yet identified, length-depth-width scaling for fractures (Schultz and Fossen, 2002) implies that the thin portions of dykes observed at the surface correspond to significantly thicker dykes at depth.

It is striking, however, that dyke dilation seems to be in great part achieved by silicic dykes, which are usually not reported in other dyke swarms associated with LIPs, which are exclusively basaltic (e.g. Ernst et al., 1995). Silicic dykes have been observed in the Serpent-God dyke swarm only, which formed above a ductile shear zone. Peculiar conditions of crustal melting in this setting might explain this particularity. For instance, water circulation is made easier in the shear zones than in the surrounding basement rocks due to a higher permeability, and may have lowered the solidus in the shear zones.

5.2. Considerations on the Ethiopian mantle plume

Both dyke swarms follow weakness zones inherited from the Precambrian that we have identified and discussed in this paper. Similar basement structural control on dyke emplacement has also been reported for the much larger Okavango Karoo dyke swarm by Le Gall et al. (2002). One of the swarms is 30 Ma old and contributed to feeding the Trap Series, and there is a good probability that the second has the same age. Dykes are thought to follow the trajectory of the maximum horizontal principal stress (Stevens, 1911; Johnson, 1970; Koide and Bhattacharji, 1975; Muller and Pollard, 1977; Mériaux and Lister, 2002), at least at regional scale (Baer et al., 1994). Since the two dyke swarms are adjacent, the stress source must be able to vary spatially at a very local scale. This probably rules out plate-boundary and related processes (Zoback, 1992). In a mantle plume setting, stress orientation is expected to be at least partly influenced by the axisymmetric plume geometry, or by pressurised magma centres (McKenzie et al., 1992; Mériaux and Lister, 2002). In the current state of the art, no evidence for more than a single axisymmetric stress source playing a role in the orientation of the studied dykes can be taken into account, because feeding magma chambers for the 30-Ma-old magmatism have not been identified yet. In the Tana–Belaya area, the short-wavelength gravity coverage is presently too sparse to help locate possible feeding magma chambers.

An example of a model of dyke emplacement in which the stress field in the study area is primarily a consequence of a single, axisymmetric source such as a mantle plume head or a large magma chamber is proposed in Fig. 13. This model ac-

counts for dyke location and geometry, influence of inherited crustal fabric, and requirement that dyke orientation reflects principal stress trajectories.

Fig. 13 also display the outline of the present-day regional Bouguer gravity anomaly in Ethiopia after Makris and Ginzburg (1987), interpreted by Rapolla et al. (1995) as due to dynamic uplift of the continental lithosphere and ascent of low-density plume material. The size of the anomaly cannot be explained by the volcanic activity that took place between the Miocene and the present, which is expressed in the residual Bouguer anomaly (Makris and Ginzburg, 1987, fig. 9). Thus, the low-density material probably dates back to the beginning of the plume activity and has drifted with the African plate, without moving with respect to the plate (Sleep, 1994). The regional gravity anomaly coincides with the western edge of a zone of negative anomalies of shear wave velocity in the mantle that extends between 100 and 250 km depth (Ritsema and van Heijst, 2000). This anomaly has been interpreted as the upper part of a hot, buoyant plume rooted beneath South Africa at 2000 km depth and inclined northward (Gurnis et al., 2000), maybe as a result of the mantle flow imposed by the motion of the African plate (Ni et al., 2002).

The gravity data reported in Fig. 13 clearly show the influence of the NE–SW Precambrian fabric on deep mass distribution. If the rising plume was cylindrical in shape and resulted in an initially axisymmetric stress field, the zone of partial melting would have initially occupied a circular zone in plan view (e.g. Watson and McKenzie, 1991). The heating and melting zones would then have propagated along the major NW–SE weakness zone. The Tulu Dimtu shear zone was not reactivated in extension prior to the volcanic activity of the Ethiopian plume, so that it would have been a preferential zone of dyke intrusion, but would not have channelled the heat and the generated magmas from the centre of the plume as efficiently as the NW–SE weakness zone would have, following the mechanism described by Ebinger and Sleep (1998) for the Ethiopian plume.

New insights on dyke emplacement have been offered in this study by the joint analysis of dyke swarm geometry, basement heterogeneity, and the ambient stress field. A well-known factor that governs dyke distribution anisotropy in LIPs is the interaction between the stress generated at the injection centre and other stress fields, such as from other injection centres or plate-boundary processes; this paper illustrates that dyke distribution at regional scale may also be primarily controlled by basement heterogeneity.

Acknowledgements

This work was funded by the CNRS/INSU 'Intérieur de la Terre' programme and involved cooperation between Pierre and Marie Curie University, Paris, and the Addis Ababa University. Hervé Diot participated in the 2002 field work and is appreciated for constantly fruitful discussing the data. The authors are indebted to Jean Chorowicz for his pioneering work in the study area, which motivated the present work. Paul Mohr is thanked for critical reading of the first draft of the manuscript, and Henry Halls and Editor Lionel Wilson for helping clarify its objectives.

References

Abbate, E., Sagri, M., 1969. Dati e considerazioni sul margine orientale dell'altppiano ethiopico nelle province del Tigrai e del Wollo. Boll. Soc. Geol. Ital. 88, 489–497.

Abdelsalam, M.G., Stern, R.J., 1996. Sutures and shear zones in the Arabian–Nubian shield. J. Afr. Earth Sci. 23, 289–310.

Adamson, D., Williams, F., 1980. Structural geology, tectonics and the control of drainage in the Nile basin: Quaternary environments and prehistoric occupation in northern Africa. In: Williams, M.A.J., H. Faure (Eds.), The Sahara and the Nile. Balkema, Rotterdam, pp. 225–252.

Ayalew, D., Yirgu, G., 2003. Crustal contribution to the genesis of Ethiopian plateau rhyolitic ignimbrites: Basalt to rhyolite geochemical provinciality. J. Geol. Soc. Lond. 160, 47–56.

Bader, C., 2000. Mythes et légendes de la Corne de l'Afrique. Khartala, Paris, 282 pp.

Baer, G., 1995. Fracture propagation and magma flow in segmented dykes: Field evidence and fabric analyses, Makhtesh Ramon, Israel. In: Baer, G., Heimann, A. (Eds.), Physics and Chemistry of Dykes. Balkema, Rotterdam, pp. 125–140.

Baer, G., Reches, Z., 1991. Mechanics of emplacement and tectonic implications of the Ramon dike system, Israel. J. Geophys. Res. 96, 11895–11910.

Baer, G., Beyth, M., Reches, Z., 1994. Dikes emplaced into fractured basement, Timna igneous complex, Israel. J. Geophys. Res. 99, 24039–24050.

Baker, B.H., Mohr, P.A., Williams, L.A.J., 1972. Geology of the Eastern Rift System of Africa. Geol. Soc. Am. Spec. Pap. 136, 67 pp.

Baragar, W.R.A., Ernst, R.E., Hulbert, L., Peterson, T., 1996. Longitudinal petrochemical variation in the Mackenzie dyke swarm, north-western Canadian shield. J. Petrol. 37, 317–359.

Berhe, S.M., 1990. Ophiolites in Northeast and East Africa: Implications for Proterozoic crustal growth. J. Geol. Soc. Lond. 147, 41–57.

Beyth, M., 1991. 'Smooth' and 'rough' propagation of spreading Southern Red Sea – Afar depression. J. Afr. Earth Sci. 13, 157–171.

Bosworth, 1992. Mesozoic and early Tertiary rift tectonics in East Africa. Tectonophysics 209, 115–137.

Bosworth, W., Strecker, M.R., 1997. Stress field changes in the Afro–Arabian rift system during the Miocene to Recent period. Tectonophysics 278, 47–62.

Braathen, A., Grenne, T., Selassie, M.G., Worku, T., 2001. Juxtaposition of Neoproterozoic units along the Baruda–Tulu Dimtu shear-belt in the East African orogen of western Ethiopia. Precamb. Res. 107, 215–234.

Cadman, A.C., 1994. The Petrogenesis and Emplacement of Proterozoic Dyke Swarms, part 2. Geochemical Processes and Paleostress Analysis. Current Res., Newfoundland Dept. of Mines and Energy, Geol. Surv. Branch, Rep. 91-1, pp. 179–190.

Callot, J.-P., Geoffroy, L., Aubourg, C., Pozzi, J.-P., Mège, D., 2001. Magma flow in shallow dykes from the E-Greenland margin inferred from magnetic fabric studies. Tectonophysics 335, 313–329.

Chorowicz, J., Collet, B., Bonavia, F.F., Mohr, P., Parrot, J.-F., Korme, T., 1998. The Tana basin, Ethiopia: Intraplateau uplift, rifting and subsidence. Tectonophysics 295, 351–367.

Coblentz, D.D., Sandiford, M., 1994. Tectonic stress in the African plate: Constraints on the ambient lithospheric stress state. Geology 22, 831–834.

Comucci, P., 1950. Le vulcaniti del lago Tana (Africa Orientale). Acad. Naz. Lincei, Roma, 209 pp.

Coulié, E., Quidelleur, X., Gillot, P.-Y., Courtillot, V., Lefèvre, J.-C., Chiesa, S., 2003. Comparative K–Ar and Ar/Ar dating of Ethiopian and Yemenite Oligocene volcanism: Implications for timing and duration of the Ethiopian traps. Earth Planet. Sci. Lett. 206, 477–492.

Ebinger, C.J., Sleep, N.H., 1998. Cenozoic magmatism throughout east Africa resulting from impact of a single plume. Nature 395, 788–791.

Ernst, R.E., Baragar, W.R.A., 1992. Evidence from magnetic fabric for the flow pattern in the Mackenzie giant radiating dyke swarm. Nature 356, 511–513.

Ernst, R.E., Buchan, K.L., Palmer, H.C., 1995. Giant dyke swarms: Characteristics, distribution and geotectonic applications. In: Baer, G., Heimann, A. (Eds.), Physics and Chemistry of Dykes. Balkema, Rotterdam, pp. 3–21.

Ernst, R.E., Grosfils, E.B., Mège, D., 2001. Giant dyke swarms: Earth, Venus and Mars. Ann. Rev. Earth Planet. Sci. 29, 489–534.

Féraud, G., Giannerini, G., Campredon, R., 1987. Dyke swarms as paleostress indicators in areas adjacent to continental collision zones: Examples from the European and north-western Arabian plates. In: Halls, H.C., Fahrig, W.F. (Eds.), Mafic Dyke Swarms. Geol. Assoc. Can. Spec. Pap. 34, pp. 273–278.

George, R., Rogers, N., Kelley, S., 1998. Earliest magmatism in Ethiopia: Evidence for two mantle plumes in one flood basalt province. Geology 26, 923–926.

Grosfils, E., Head, J.W., 1994. The global distribution of giant radiating dike swarms on Venus: Implications for the global stress state. Geophys. Res. Lett. 21, 701–704.

Gudmundsson, A., 1984. Tectonic aspects of dykes in northwestern Iceland. Jökull 34, 81–96.

Gudmundsson, A., 1987. Tectonics of the Thingvellir fissure swarm, SW Iceland. J. Struct. Geol. 9, 61–69.

Gurnis, M., Mitrovica, J.X., Ritsema, J., van Heijst, H.-J., 2000. Constraining mantle density structure using geological evidence of surface uplift rates: The case of the African superplume. Geophys. Geochem. Geosyst. 1, 1999 GC000035.

Hahn, G.A., Raynolds, R.G.H., Wood, R.A., 1977. The geology of the Angareb ring dike complex, north-western Ethiopia. Bull. Volcanol. 40, 1–10.

Hart, W.K., Woldegabriel, G., Walter, R.C., Mertzman, S.A., 1989. Basaltic volcanism in Ethiopia: Constraints on continental rifting and mantle interactions. J. Geophys. Res., 94, 7731–7748.

Hofmann, C., Courtillot, V., Féraud, G., Rochette,.P., Yirgu, G., Ketefo, E., Pik, R., 1997. Timing of the Ethiopian flood basalt event and implications for plume birth and global change. Nature 389, 838–841.

Ibrahim, A.E., Ebinger, C.J., Fairhead, J.D., 1996. Lithospheric extension north-west of the Central African Shear Zone in Sudan from potential field studies. Tectonophysics 255, 79–97.

Jaeger, J.C., 1968. Cooling and solidification of igneous rocks. In: Hess, H.H., Poldervaart, A. (Eds.), Basalts, the Poldervaart Treatise on Rocks of Basaltic Composition, vol. 2. Wiley and Sons, New York, pp. 503–536.

Jepsen, D.H., Athearn, 1961. The Geology of Ethiopia. Univ. College Addis Ababa Press, Addis Ababa.

Jepsen, D.H., Athearn, B.M.J., 1962. East–West Geologic Sections, Blue Nile River Basin. Eth. Dept. Water Res., Addis Ababa, 5.2-BN-3.

Jepsen, D. H., Athearn, B.M.J., 1963a. General Geology Reconnaissance Map, Vicinity of Ismale Georgis. Eth. Dept. Water Res., Addis Ababa, 5.2-LT-3.

Jepsen, D.H., Athearn, B.M.J., 1963b. Blue Nile Basin Report. Eth. Dept. Water Res., Addis Ababa, 67 pp.

Johnson, A.M., 1970. Physical Processes in Geology. Freeman, 577 pp.

Jordan, R., 1972. The Jurassic of north-eastern Ethiopia. In: Canuti, P., Greguanin, A., Piccirillo, E.M., Sagri, M., Tacconi, P. (Eds.), Volcanic Intercalation in the Mesozoic Sediments of the Kulubi Area (Harar, Ethiopia). Bull. Soc. Geol. Ital. 91, 92–95.

Justin-Visentin, E., Zanettin, B., 1974. Dike swarms, volcanism and tectonics of the western Afar margin along the Kombolcha–Eloa traverse (Ethiopia). Bull. Volcanol. 38, 187–205.

Kazmin, V., 1975. Explanation of the Geological Map of Ethiopia. Geol. Surv. Eth., Addis Ababa, 14 pp.

Kazmin, V., Shifferaw, A., Balcha, T., 1978. The Ethiopian basement: Stratigraphy and possible manner of evolution. Geol. Rundsch. 67, 531–546.

Kennan, P.S., Mitchell, J.G., Mohr, P., 1990. The Sagatu ridge dyke swarm, Ethiopian rift margin: Revised age and new Sr-isotopic data. J. Afr. Earth Sci. 11, 39–42.

Koide, H., Bhattacharji, S., 1975. Formation of fractures around magmatic intrusions and their role in ore localization. Econ. Geol. 70, 781–799.

Lachenbruch, A.H., 1962. Mechanics of Thermal Contraction Cracks and Ice-Wedge Polygons in Permafrost. Geol. Soc. Am. Sped. Pap. 70, 69 pp.

Le Gall, B., Tshoso, G., Jourdan, F., Féraud, G., Bertrand, H., Tiercelin, J.J., Kampunzu, A.B., Modisi, M.P., Dyment, J., Maia, M., 2002. $^{40}Ar/^{39}Ar$ geochronology and structural data from the giant Okavango and related mafic dyke swarms, Karoo igneous province, northern Botswana. Earth Planet. Sci. Lett. 202, 595–606.

Lebas, M.J., Mohr, P.A., 1970. Tholeiite from the Simien alkali basalt centre, Ethiopia. Geol. Mag. 107, 523–529.

Makris, J., Ginzburg, A., 1987. The Afar Depression: Transition between continental rifting and sea-floor spreading. Tectonophysics 141, 199–214.

Marty, B., Pik, R., Yirgu, G., 1996. Helium isotopic variations in Ethiopian plume lavas: Nature of magmatic sources and limit of lower mantle contribution. Earth Planet. Sci. Lett. 144, 223–237.

May, P.R., 1971. Pattern of Triassic–Jurassic diabase dikes around the North Atlantic in the context of predrift position of the continents. Geol. Soc. Am. Bull. 82, 1285–1292.

McKenzie, D., McKenzie, J.M., Saunders, R.S., 1992. Dike emplacement on Venus and on Earth. J. Geophys. Res. 97, 15977–15990.

Mège, D., Korme, T., 2004. Fissure eruption of flood basalts from statistical analysis of dyke fracture length. J. Volcanol. Geotherm. Res. 131, 77–92.

Mège, D., Masson, P., 1996. A plume tectonics model for the Tharsis province, Mars. Planet. Space Sci. 44, 1499–1546.

Merla, G., Abbate, E., Azzaroli, A., Bruni, P., Canuti, P., Fazzuoli, M., Sagri, M., Tacconi, P., 1979. A Geologic Map of Ethiopia and Somalia (1973), 1:2,000,000, and Comment with a Map of Major Landforms. Cons. Naz. Ric. Ital., Firenze, 95 pp.

Mériaux, C., Lister, J.R., 2002. Calculation of dike trajectories from volcanic centers. J. Geophys. Res. 107, 10.1029/2001-JB000436.

Mohr, P., 1963. The Ethiopian Cainozoic lavas, a preliminary study of some trends: Spatial, temporal, and chemical. Bull. Geophys. Obs. Addis Ababa 6, 103–144.

Mohr, P., 1967. Review of the geology of the Simien Mountains. Bull. Geophys. Obs. Addis Ababa 10, 79–93.

Mohr, P., 1971. Ethiopian Tertiary Dyke Swarms. Smithson. Astrophys. Obs. Spec. Rep., 339, 53 pp.

Mohr, P., 1980. Geochemical aspects of the Sagatu ridge dike swarm, Ethiopian rift margin. In: Geodynamic Evolution of the Afro–Arabian Rift System. Acad. Nat. Lincei, Atti Convegni Lincei 47, pp. 384–067.

Mohr, P., 1983. The Morton–Black hypothesis for the thinning of continental crust – revised in western Afar. Tectonophysics 94, 509–528.

Mohr, P., 1999. The Asmara dike swarm, Eritrean plateau: Physical parameters of an off-rift olivine dolerite injection zone. Acta Vulcanol. 11, 177–181.

Mohr, P., Potter, E.C., 1976. The Sagatu ridge dike swarm, Ethiopian rift margin. J. Volcanol. Geotherm. Res. 1, 55–71.

Mohr, P., Zanettin, B., 1988. The Ethiopian flood basalt province. In: McDougall, J.D. (Ed.), Continental Flood Basalts. Kluwer, Dordrecht, pp. 63–110.

Muller, O.H., Pollard, D.D., 1977. The state of stress near Spanish Peaks, Colorado, determined from a dike pattern. Pure Appl. Geophys. 115, 69–86.

Ni, S., Tan, E., Gurnis, M., Helmberger, D., 2002. Sharp sides to the African superplume. Science 296, 1850–1852.

Ohnenstetter, D., Brown, W.L., 1992. Overgrowth textures, disequilibrium zoning, and cooling history of a glassy four-pyroxene boninite dyke from New Caledonia. J. Petrol. 33, 231–271.

Pik, R., Deniel, C., Coulon, C., Yirgu, G., Hofmann, C., Ayalew, D., 1998. The northwestern Ethiopian Plateau flood basalts: Classification and spatial distribution of magma types. J. Volcanol. Geotherm. Res. 81, 91–111.

Pik, R., Deniel, C., Coulon Hofmann, C., Yirgu, G., Marty, B., 1999. Isotopic and trace element signatures of Ethiopian flood basalts: Evidence for plume-lithosphere interactions. Geochim. Cosmochim. Acta 63, 2263–2279.

Platten, I.M., 2000. Incremental dilation of magma filled factures: Evidence from dykes on the Isle of Skye, Scotland. J. Struct. Geol. 22, 1153–1164.

Purcell, P.G., 1976. The Marda Fault Zone, Ethiopia. Nature 261, 569–571.

Rapolla, A., Cella, F., Dorre, A.S., 1995. Moho and lithosphere–asthenosphere boundaries in East Africa from regional gravity data. Boll. Geofis. Teor. Apl. 37, 277–301.

Ritsema, J., van Heijst, H., 2000. New seismic model of the upper mantle beneath Africa. Geology 28, 63–66.

Salama, R.B., 1997. Rift basins in Sudan. In: Selley, R.C. (Ed.), African Basins. Sedimentary Basins of the World, vol. 3, Elsevier, Amsterdam, pp. 105–149.

Schultz, R.A., Fossen, H., 2002. Displacement-length scaling in three dimensions: The importance of aspect ratio and

application to deformation bands. J. Struct. Geol. 24, 1389–1411.

Shackleton, R.M., 1979. Precambrian tectonics of North-East Africa. In: al-Ashanti, A.M.S. (Ed.), Evolution and Mineralization of the Arabian–Nubian Shield, vol. 2. I.A.G. Bull. 3, Pergamon Press, 1–6.

Shackleton, R.M., 1986. Precambrian collision tectonics in Africa. In: Coward, M.P., Ries, A.C. (Eds.), Collision Tectonics. Geol. Soc. Spec. Publ. 19, pp. 329–349.

Shackleton, R.M., 1988. Contrasting structural relationships of Proterozoic ophiolites in Northeast and Eastern Africa. In: el-Gaby, S., Greiling, R.O. (Eds.), The Pan-African Belt of Northeast Africa and Adjacent Areas. Vieweg, Wiesbaden, pp. 183–193.

Sleep, N.H., 1994. Lithospheric thinning by midplate mantle plumes and the thermal history of hot plume material ponded at sublithospheric depths. J. Geophys. Res. 99, 9327–9343.

Stern, R.J., 1994. Arc assembly and continental collision in the Neoproterozoic east African orogen. Ann. Rev. Earth Planet. Sci. 22, 319–351.

Stern, R.J., Nielsen, K.C., Best, E., Sultan, M., Arvidson, R.E., Kröner, A., 1990. Orientation of late Precambrian sutures in the Arabian–Nubian shield. Geology 18, 1103–1106.

Stevens, B., 1911. The laws of intrusion. Bull. Am. Inst. Mining Eng. 49, 1–25.

Stewart, K., Rogers, N., 1996. Mantle plume and lithosphere contributions to basalts from southern Ethiopia. Earth Planet. Sci. Lett. 139, 195–211.

Swanson, D.A., Wright, T.L., Helz, R.T., 1975. Linear vent systems and estimated rates of magma production and eruption of the Yakima basalt on the Columbia Plateau. Am. J. Sci. 275, 877–905.

Tadesse, T., 1996. Structure across a possible intra-oceanic suture zone in the low-grade Pan-African rocks of northern Ethiopia. J. Afr. Earth Sci. 23, 375–381.

Takada, A., 1994. Accumulation of magma in space and time by crack interaction. In: Ryan, M.P. (Ed.), Magmatic Systems. Academic Press, pp. 241–257.

Tessema, A., Antoine, L.A.G., 2003. Variation in effective plate thickness of the East Africa lithosphere. J. Geophys. Res. 108, 10.129/2002JB002200.

Thompson, R.N., Gibson, S.A., 1991. Subcontinental mantle plumes, hotspots and pre-existing thinspots. J. Geol. Soc. Lond. 148, 973–977.

Touchard, Y., Rochette, P., Aubry, M.-P., Michard, A., 2003. High-resolution magnetostratigraphic and biostratigraphic study of Ethiopian traps-related products in Oligocene sediments from the Indian ocean. Eart Planet. Sci. Lett. 206, 493–508.

Vail, J.R., 1976. Outline of the geochronology and tectonic units of the basement complex of North East Africa. Proc. R. Soc. Lond. A 350, 127–141.

Vail, J.R., 1985. Pan-African (late Precambrian) tectonic terrains and the reconstruction of the Arabian–Nubian shield. Geology 13, 839–842.

Wada, Y., 1992. Magma flow directions inferred from preferred orientations of phenocryst in a composite feeder dike, Miyake-Jima, Japan. J. Volcanol. Geotherm. Res. 49, 119–126.

Wada, Y., 1994. On the relationship between dike width and viscosity. J. Geophys. Res. 99, 17743–17755.

Watson, S., McKenzie, D., 1991. Melt generation by plumes: A study of Hawaiian volcanism. J. Petrol. 32, 501–537.

Wilson, L., Head, J.W., 1994. Mars: review and analysis of volcanic eruption theory and relationships to observed landforms. Reviews of Geophysics 32(3), 221-263.

Zanettin, B., Justin-Visentin, E., 1974. The Volcanic Succession in Central Ethiopia, 2. The Volcanics of the Western Afar and Ethiopian Rift Margins. Centr. Stud. Geol. Petrol. Formazioni Cristalline, CNR, Padova, 19 pp.

Zoback, M.L., 1992. First- and second-order patterns of stress in the lithosphere: The World Stress Map project. J. Geophys. Res. 97, 11703–11728.